

UC Irvine

UC Irvine Previously Published Works

Title

Calibration techniques for fast-ion D α diagnostics.

Permalink

<https://escholarship.org/uc/item/00t3w1qw>

Journal

The Review of scientific instruments, 83(10)

ISSN

0034-6748

Authors

Heidbrink, WW
Bortolon, A
Muscatello, CM
[et al.](#)

Publication Date

2012-10-01

DOI

10.1063/1.4732060

Copyright Information

This work is made available under the terms of a Creative Commons Attribution License, available at <https://creativecommons.org/licenses/by/4.0/>

Peer reviewed

Calibration techniques for fast-ion D_α diagnostics^{a)}

W. W. Heidbrink,^{1,b)} A. Bortolon,¹ C. M. Muscatello,¹ E. Ruskov,¹ B. A. Grierson,²
and M. Podestá²

¹University of California, Irvine, California 92697, USA

²Princeton Plasma Physics Laboratory, Princeton, New Jersey 08543, USA

(Presented 8 May 2012; received 10 May 2012; accepted 6 June 2012;
published online 3 July 2012)

Fast-ion D_α measurements are an application of visible charge-exchange recombination (CER) spectroscopy that provide information about the energetic ion population. Like other CER diagnostics, the standard intensity calibration is obtained with an integrating sphere during a vacuum vessel opening. An alternative approach is to create plasmas where the fast-ion population is known, then calculate the expected signals with a synthetic diagnostic code. The two methods sometimes agree well but are discrepant in other cases. Different background subtraction techniques and simultaneous measurements of visible bremsstrahlung and of beam emission provide useful checks on the calibrations and calculations. © 2012 American Institute of Physics. [<http://dx.doi.org/10.1063/1.4732060>]

I. INTRODUCTION

Fast-ion D_α (FIDA) diagnostic technique exploits the Doppler shift of the Balmer-alpha emission from neutralized deuterons to obtain velocity and profile information about the fast-ion distribution function.¹ This paper focuses on methods to assess the validity of the intensity calibration.

The primary intensity calibration during a vacuum opening follows a standard procedure. Each optical fiber is backlit, then the aperture of a calibrated integrating sphere is positioned to intersect the light cone of the illuminated fiber. After the fiber is reconnected to the spectrometer, the camera measures the number of counts produced by the source, providing a calibration factor that relates counts to the absolute spectral radiance. Usually this intensity calibration is performed both before and after experimental campaigns, since tokamak operation can degrade optical components.

A calibration during physics operations requires a known source. A common approach is to attempt to produce a known fast-ion distribution function by injecting neutral beams into an MHD-quiescent plasma. For such conditions a code such as TRANSP NUBEAM (Ref. 2) can accurately model the distribution function. The NUBEAM distribution function is input to a synthetic diagnostic code such as FIDASIM (Ref. 3) that calculates the expected FIDA spectral radiance for use as a calibration reference. Agreement (to within ~25%) between theory and experiment have been reported for spectrometers at DIII-D (Ref. 4) and ASDEX-Upgrade.⁵

In other cases, the predicted signal disagrees with the measurement. There are many possible causes of a discrepancy, including measurement errors (particular background subtraction), errors in beam parameters (power, species mix, spatial profile), errors in plasma parameters (which affect calculations of injected neutral beam, halo, and fast-ion densities), and modeling errors. The latter include programming

“bugs” such as ones that were recently identified in the FIDASIM code (the comparisons in this paper are from IDL version 4.0) and deficiencies in the NUBEAM model such as the neglect of fast-ion transport by instabilities. Using recently analyzed NSTX and DIII-D cases as examples, this paper presents several additional comparisons that can confirm or eliminate some of these potential sources of error.

II. NSTX VERTICAL FIDA EXAMPLE

The NSTX vertically-viewing s-FIDA diagnostic⁶ uses a transmission grating spectrometer in conjunction with a CCD camera to measure D_α spectra between 645–667 nm. An OD2 neutral density filter in the spectrometer image plane partially blocks the bright, cold D_α centerline. One set of active fibers views a heating beam, while a similar set of toroidally displaced fibers provides reference views.

In 2008 and 2009, a set of experiments were conducted to check the calibration and modeling of the FIDA emission. To minimize MHD activity, a single modulated (50 Hz at 50% duty cycle) 65 keV neutral beam was injected into plasmas with different values of plasma current I_p , density n_e , and toroidal field B_T . Of the beam-driven instabilities that are commonly observed in NSTX, low-frequency instabilities such as the toroidal Alfvén eigenmode (AE) were absent but, despite the low beam power, MHz global or compressional AEs were present in these discharges. The measured neutron rate agrees well with TRANSP predictions during the low-power phase, suggesting that any spatial transport caused by the MHz instabilities is modest.

Figure 1 shows raw and calibrated spectra from a representative spatial channel. For the channel that views the beam, a FIDA feature is obviously present on the blueshifted wing of the D_α line (652–655 nm) (Fig. 1(a)). As expected, the FIDA feature is absent in the spectrum from the toroidally displaced fiber (Fig. 1(b)). Other features in the spectra are associated with impurity lines and with the attenuation caused by the neutral-density filter. Figure 1(c) shows the “beam-off”

^{a)}Contributed paper, published as part of the Proceedings of the 19th Topical Conference on High-Temperature Plasma Diagnostics, Monterey, California, May 2012.

^{b)}Electronic mail: bill.heidbrink@uci.edu.

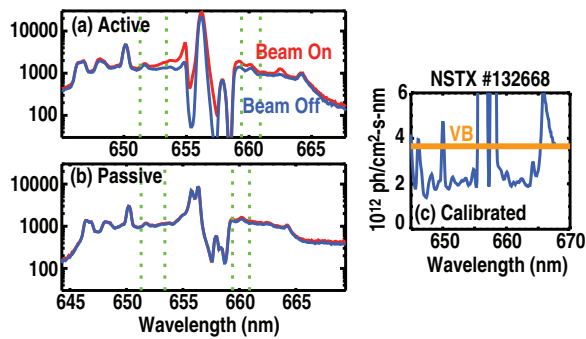


FIG. 1. Raw data from (a) active and (b) reference channels near $R = 120$ cm. The “beam on” and the “beam off” signals differ on the wings of the central line (656.1 nm) for the active view but not for the reference view. (c) Calibrated spectrum from the active channel when the beam is off. The calibrated spectrum is ~ 2 times smaller than the calculated VB emission.

active spectrum after application of the calibration factors. The spectrum is reasonable. The central D_α line is very bright. Impurity lines, such as the oxygen V line at 650.0 nm, rise above a fairly flat background.

The spectral intensity of visible bremsstrahlung (VB) is essentially constant between 645–670 nm and provides a convenient check on the intensity calibration. It is straightforward to calculate the expected VB level from the plasma profiles and diagnostic sightlines used in the FIDASIM code. The code neglects any emission from outside the last-closed flux surface, so the measured background should be \gtrsim the calculated VB. The data in Fig. 1(c) fail this test, strongly suggesting that the intensity calibration underestimates the true intensity by a factor of ~ 2 . The error source is currently unknown.

Another useful check is to compare methods of background subtraction. The data should satisfy the following criteria. (1) The net spectra should go to zero at large Doppler shifts. (2) The spectrum derived from beam modulation (“beam on – beam off”) should equal the spectrum derived from the reference view (“active view – reference view”). (3) For a reference view, the beam modulation spectrum (“beam on – beam off”) should be flat and approximately zero. Figure 2 shows comparisons of this type for a representative spatial channel. For this channel, the blueshifted spectra meet all three criteria but the redshifted spectra do not. In particular, the redshifted beam-modulation spectrum is > 0 at large Doppler shift (661–662 nm), the spectra derived from the two background-subtraction techniques differ, and the reference background is larger when the diagnostic beam is on than when it is off. Similar comparisons for the other spatial channels show that the validity of the blueshifted and redshifted spectra depends upon position. An investigation suggests that the errors in background subtraction are caused by scattered light. The spectra are measured in three bands: large blueshift I_B , cold D_α line I_C , and large redshift I_R . The “large” blue and redshifts are for Doppler shifts greater than the injection energy. A database shows that the baseline offsets I_B and I_R are both strongly correlated with the cold intensity I_C .

Some aspects of the FIDASIM predictions disagree with the data while others agree. The overall intensity is discrepant for all channels. The observed spatial profile shape is $\sim 30\%$

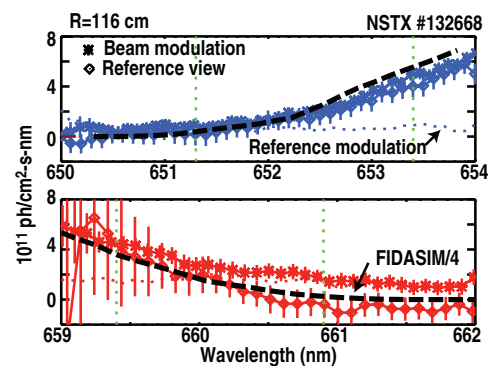


FIG. 2. Comparison of background subtraction techniques for spectra from the $R = 116$ cm channel. The background subtraction utilizes either beam modulation (*) or the passive reference view (\diamond). The dotted line shows the temporal variation of the reference view (beam on – beam off). The dashed line is the prediction from FIDASIM after division by 4.

broader than theory. On the other hand, the spectral shape is in excellent agreement with theory for all channels. The parametric dependencies of the signals also agree with theory. To test this, the maximum measured and calculated radiance is measured for all 12 discharges in the dedicated experiment for both the blueshifted and the redshifted side of the spectrum. The correlation coefficient between theory and experiment is $r \approx 0.9$ for both sides of the spectrum.

To summarize, although the vertical NSTX FIDA diagnostic unquestionably is measuring FIDA light, the absolute intensity calibration is suspect. At this point, calibration errors, errors in beam parameters, and modeling errors all remain candidates to explain the discrepancy.

III. DIII-D EXAMPLES

DIII-D is currently equipped with three spectroscopic FIDA diagnostics with vertical, oblique, and tangential views of the plasma. The vertically-viewing profile diagnostic employs a Czerny–Turner spectrometer tuned to the blue side of the cold D_α line. The obliquely-viewing diagnostic⁷ employs a transmission grating spectrometer that only measures the blueshifted side of the spectrum. A bandpass filter transmits the blue wing but strongly attenuates the cold D_α line. The main-ion CER diagnostic⁸ measures the entire D_α feature with a pair of tangential views. It employs a Czerny–Turner spectrometer and a 12-bit CCD camera. For FIDA measurements, the pixels at the cold D_α line are allowed to saturate weakly. (“Weak” saturation occurs for signals that are less than about twice the full well depth.) When weak saturation happens, the spectra are merely clipped over a few (2–5) pixels and other pixels appear unaffected. (In contrast, for stronger saturation, the entire register (128 pixels) associated with the saturated pixels will exhibit a baseline “sag”; these spectra are unusable.) The analysis procedure fits the entire spectrum.⁸ All three diagnostics normally use beam modulation to remove the background.

Figure 3 shows analyzed main-ion CER data following injection for 100 ms of a single 74 keV, 2.2 MW source. The diagnostic beam is pulsed on for 10 ms. Figure 3(a) compares the spatial profile of the fitted beam emission spectra for the

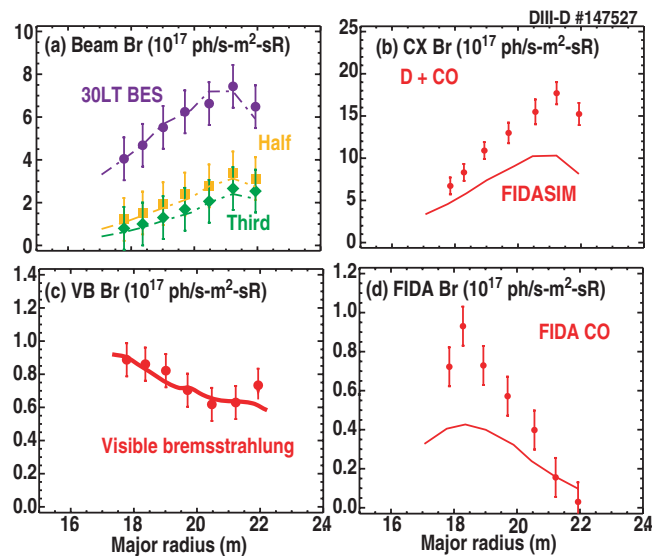


FIG. 3. Measured (symbols) and predicted (lines) profiles for the DIII-D main-ion CER diagnostic for channels that view a co-going diagnostic beam. (a) Beam emission, (b) thermal deuterium feature from direct charge exchange and halo neutrals, (c) VB between 660 nm and 662 nm, (d) FIDA feature.

full, half, and third-energy components with the brightness predicted by FIDASIM. The agreement is excellent. The first FIDA diagnostics intentionally avoided the beam emission in their design¹ but the data from the main-ion CER diagnostic show that it is preferable to measure beam emission as well as the FIDA feature. The good agreement between theory and experiment shown in Fig. 3(a) confirms that the injected neutral density is accurately modeled, eliminating one potential source of error in the modeling.

The calculated VB level is in excellent agreement with the observed background at large Doppler shifts for this instrument (Fig. 3(c)). Only the outermost channel shows a significant discrepancy, owing to reflections off a metallic surface that is in its sightline. The excellent agreement confirms the validity of the experimental calibration and of the modeling of the plasma profiles for this discharge.

The halo of thermal neutrals that surround the injected beam also contribute to the charge-exchange events that produce FIDA light. Figure 3(b) shows the profile of light produced by thermal deuterons. The discrepancy between the measured and calculated deuteron brightness suggests that the halo density is underestimated by FIDASIM. Alternatively, the geometry of the neutral beam may be specified incorrectly. Similarly, the shape of the spatial profile agrees well with

FIDASIM predictions but the magnitude differs (Fig. 3(d)), probably because FIDASIM is underestimating the halo neutral density.

To create a calibration discharge for the vertical and oblique diagnostics, a single steady 60 keV beam injected 1.3 MW into an L-mode discharge with negligible MHD activity. The measured neutron rate is in excellent agreement with the rate predicted by TRANSP, suggesting that the fast-ion distribution function is accurately modeled. For both of these diagnostics, the predicted VB signal is about a factor of two smaller than the apparent baseline. This probably indicates that scattered light is increasing the background level. A laboratory calibration experiment⁹ indicates that scattered light is a problem for the transmission-grating spectrometer design.

The spectral shape predicted by FIDASIM is in excellent agreement with the measurements for both diagnostics. The magnitude of the FIDA signal also agrees reasonably well with the predictions for both systems, although the spatial profile shape is only in fair agreement with theory.

These examples illustrate the power of comparing the data with as many spectral features as possible. Each successful comparison eliminates potential sources of error, while unsuccessful comparisons highlight likely sources of error.

ACKNOWLEDGMENTS

This work was funded by the U.S. Department of Energy (DOE) under Grant Nos. SC-G903402, DE-FC02-04ER54698, DE-FG03-02ER54681, and DE-FG02-06ER54867. We thank R. Akers, B. Geiger, D. Liu, C. Michael, and D. C. Pace for helpful suggestions and acknowledge the support of the NSTX and DIII-D experimental teams, particularly Ron Bell at NSTX and the CER group at DIII-D.

¹W. W. Heidbrink, *Rev. Sci. Instrum.* **81**, 10D727 (2010).

²A. Pankin, D. Mccune, R. Andre, G. Bateman, and A. Kritiz, *Comput. Phys. Commun.* **159**, 157 (2004).

³W. W. Heidbrink, D. Liu, Y. Luo, E. Ruskov, and B. Geiger, *Comm. Comp. Phys.* **10**, 716 (2011).

⁴Y. Luo, W. W. Heidbrink, E. Ruskov, K. H. Burrell, and W. M. Solomon, *Phys. Plasmas* **14**, 112503 (2007).

⁵B. Geiger, M. Garcia-Munoz, W. W. Heidbrink *et al.*, *Plasma Phys. Controlled Fusion* **53**, 065010 (2011).

⁶M. Podesta, W. W. Heidbrink, R. E. Bell, and R. Feder, *Rev. Sci. Instrum.* **79**, 10E521 (2008).

⁷C. M. Muscatello, W. W. Heidbrink, D. Taussig, and K. H. Burrell, *Rev. Sci. Instrum.* **81**, 10D316 (2010).

⁸B. A. Grierson, K. H. Burrell, W. W. Heidbrink, N. A. Pablant, and W. M. Solomon, *Phys. Plasma* **19**, 056107 (2012).

⁹C. M. Muscatello, "Velocity-space resolved fast-ion measurements in the DIII-D tokamak," Ph.D. dissertation, University of California, Irvine, 2012.